sciendo

POLISH MARITIME RESEARCH 3 (115) 2022 Vol. 29; pp. 89-98
10.2478/pomr-2022-0029

JACKING AND ENERGY CONSUMPTION CONTROL OVER NETWORK FOR JACK-UP RIG: SIMULATION AND EXPERIMENT

Viet-Dung Do [1,2]
Xuan-Kien Dang [1] *
Tien-Dat Tran [1]
Thi Duyen-Anh Pham [1]
[1] Artificial Intelligent Transportation Research Group, Ho Chi Minh City University of Transport, Vietnam
[2] Dong An Polytechnic, Vietnam

* Corresponding author: *kien.dang@ut.edu.vn (Xuan-Kien Dang)*

ABSTRACT

Oil and gas projects differ from regular investment projects in that they are frequently large-scale, categorised as vital national projects, highly technological, and associated with significant risks. Drilling rigs are a crucial component of the oil and gas sector and the majority of the systems and equipment aboard drilling rigs are operated automatically. Consequently, it is crucial to address the topic of an advanced control theory for off-shore systems. Network technology connected to control is progressively being used to replace outdated technologies, together with other contemporary technologies. In this study, we examine how to adapt a networked control jacking system to the effects of internal and external disturbances with a time delay, using a Fuzzy controller (FC)-based particle swarm optimisation. To demonstrate the benefit of the proposed approach, the developed Fuzzy Particle Swarm Optimisation (FPSO) controller is compared with the fuzzy controller. Finally, the results from simulations and experiments utilising Matlab software and embedded systems demonstrate the suitability of the proposed approach.

Keywords: Networked control system, Environmental forces, Energy consumption, Fuzzy Particle swarm optimization, Jacking system, Time-delay

INTRODUCTION

In the role of exploiting oil and gas from below the oceans, several locations are planned for numerous small-scale drilling rigs, all of which are connected to, and communicate with, one another (for example, the Dai Hung 01 and Dai Hung 02 rigs in the Vietnam's continental shelf). Typically, one rig will serve as the operations centre, fully outfitted with monitoring technology for the other dependent rigs and manned by people, as shown in Fig. 1. The other, smaller, rigs are known as 'slavers' and the majority of them are automated, being run by a central rig with no operator. Underground power lines link the slavers, the majority of which do not yet include wireless monitoring, control systems or network control. The fundamental cause of this is that the control algorithms have not encountered the safety expectations required when the system is controlled over a network. As a result, experts still attempt to remotely operate systems and equipment that are located offshore. The model must be tested and analysed in simulated environments before being applied in natural settings.

Jack-up platforms have been used for drilling, workover, and offshore oil and gas exploration for many years. In the process of jacking up a Jack-up Rig (JuR), there are numerous approaches [1-4] to controlling stability and reducing the forces that affect them. Even though each approach has its advantages, the study of intelligent control algorithms continually pushes

experts to find theoretical and practical solutions to help the system run more consistently and securely, and to carry out many more tasks than were previously conceivable. Many academics are devoted to developing improved technology and artificial intelligence because of the exceptional benefits that may be possible [5–10]. Fuzzy [5], Hybrid Fuzzy [6], Fuzzy Adaptive [7], Neural Network [8], Genetic Algorithm (GA) [9], and Particle Swarm Optimisation (PSO) [10] are a few of the recommended advanced control approaches that have demonstrated their efficacy and stability. In addition, there has been a lack of investigation into utilising existing control theory to improve the performance and efficacy of controllers, particularly complex systems or systems controlled through networks. The stability and continuity of the system is greatly influenced by time-delay and disturbances. Therefore, the method of control based on randomness also takes network technology, transmission speed, and packet drop-out data into consideration.

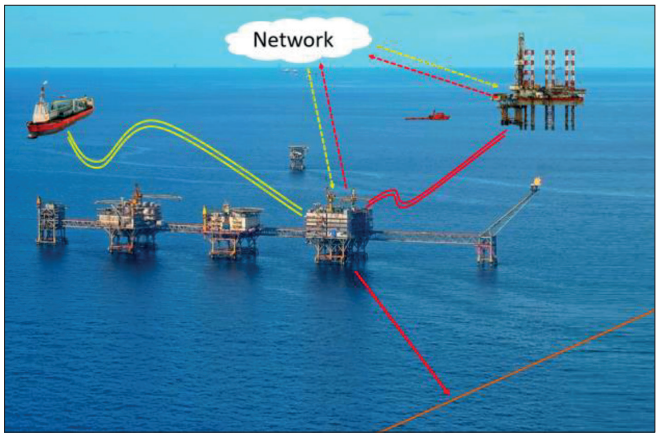

Fig. 1. The idea of network control systems for a Jack up Rig in off-shore systems

Recent literature has achieved a lot of innovative results, with respect to Fuzzy Control (FC) [6-7], which copes with problems of unpredictability, disturbance, and time-delay. This method was developed based on natural language; it can produce estimates that are more accurate and reflect the true nature of the issues. The fuzzy controller may be adjusted appropriately, and in an efficient manner, because of the use of metaheuristic algorithms, like the PSO. By using this method, the FLC may be easily adjusted to provide the appropriate performance without the need for extensive traditional testing. Within the limitations of a class of switching signals with typical dead-time, the FC technique maintains all closed-loop signals. It is also believed that the Adaptive Fuzzy Control (AFC) is a useful strategy for enhancing the performance of the fuzzy controller, particularly for Self-Adaptive Fuzzy Control (SAFC) [11–13], FPSO [14]. On the other hand, to improve the SAFC's flexibility and stability, optimum algorithms like GA and PSO are being researched and used in conjunction with fuzzy logic. Concerning networked control systems, FC is used to approximate the unknown nonlinear characteristics occurring in the system, while the Pade approximation was launched to handle network-induced delays [15]. In addition, model free fuzzy adaptive control has also been proposed for networks and, in this case, the controller can track the reference trajectory satisfactorily, even in the presence of unmeasured disturbances and network-induced time delays [16]. It should be noted that, these factors motivated us to choose to employ the innovative technique for the JuR's jacking networked system, as it must operate in difficult environmental and network conditions.

Automated controllers are not essential in the process of constructing rigs in Vietnam and networked control is also not a key issue in the study. Considering that the fuzzy system may approximate a nonlinear composition, the hierarchical fuzzy model is an excellent technique for the JuR, with unexpected effects of time-delays and disturbances. To solve the mentioned problems, we proposed the PSO-based FC to improve the performance of the JuR's jacking networked control system by simulation. However, experimental validation of the proposed controller on the model is necessary in order to deploy the research outcome to the offshore industry. The study's main contributions include the following:

(1) Developing a mathematical model of the Jacking system (JS) and incorporating it into a networked model.
(2) Outlining a networked control model with the FPSO controller, considering the fact that the conventional controller designed for the JS is not that practical in light of disturbances and time-delays, including network issues.
(3) Simulating and testing the FPSO controller in the model was contrasted with the other controller, to demonstrate the novelty of the proposed strategy.

The structure of this paper is as follows. Section 2 presents the mathematical model of the JS-included network and Section 3 analyses the factors which are already impacted, such as internal and external load and networked-induced delay. The FPSO control strategies are outlined in Section 4. Discussion of the simulation and experimental studies is presented in Section 5 and the study's concluding remarks are addressed in Section 6.

MATHEMATICAL MODEL OF THE JACKING CONTROL SYSTEM

The two most popular techniques for static or dynamic analysis of the JuR are the direct finite-element methodology [17] and the simple beam approach [18]. In the first approach, the rig is viewed as a spatial lattice frame structure with the forces and displacements in each member taken into account. In the other approach, the entire rig is replaced by a uniform beam carrying a lumped mass, designed to allow its static or dynamic behaviour to be predicted using straightforward theoretical formulas. The first technique is too complex to supply essential design knowledge, while the second is too straightforward to offer reliable information, hence neither should be used in the early phases of design. Because of this, it is simple to derive the equations of motion for the JuR by first determining the equations of motion for each leg and the upper hull separately, then integrating them, while enforcing the constraints of deformation compatibility and

force equilibrium at the intersections of the legs and the hull. Dynamic equations of motion-related topics are discussed in detail in [19–24], where the dynamic motion model is impacted by internal elements, including stress and stiffness [25], as well as environmental elements [26]. There are six degrees of freedom at each nodal point:

– Translations: heave, swing, and surge.
– Rotational: Yaw, pitch, and roll.

The uncertain elements of the structure and its surroundings may be ignored or taken into account in the analysis being used. The architecture of the inertia, damping, and stiffness matrices can be either deterministic or probabilistic. Excitation forces and subsoil layers are produced in such a system by the uncertainty of the matrix terms. The general form of the dynamic equations of motion is as follows [19]:

$$M(\chi)\ddot{q}(\chi, t) + C(\chi)\dot{q}(\chi, t) + K(\chi)q(\chi, t) = P\left(t, \dot{q}(\chi, t), \ddot{q}(\chi, t)\right) \quad (1)$$

where χ is a component in a set of fundamental actions and the mass of the surrounding water, sometimes referred to as the hydro-dynamic, related, or additional mass, is included in the global inertia matrix $M(\chi)$, which is made up of the structural mass. The three flexible continuous elements that ensure the integrity, subsoil, and water are $C(\chi)$, the global damping matrix is $K(\chi)$, and $P\left(t, \dot{q}(\chi, t), \ddot{q}(\chi, t)\right)$ is the global vector of forces brought by the wind and the waves. The common formula for six degrees of freedom that apply to all motion directions is given in Eq. (1). We are interested in the lifting-lowering motion of the jacking system in the z-direction, which means that the displacement and position are the same thing. The mismatch between the desired and the actual position is used by the controller to calculate the control signal supplied to the thrust allocation. As a result, the thrust allocation distributes the control instructions to the thruster dynamics by converting the control signal into command signals (such as the motor shaft's speed, rotational direction, and torque). Here, we set the displacement to be $p_j^\star(t)$. Eq. (1) is now equivalent to Eq. (2) [14]:

$$M\frac{d^2p_j^\star(t)}{dt^2} + C\frac{dp_j^\star(t)}{dt} + Kx(t) = \tau_{dc}(t) + \tau_d(t) \quad (2)$$

where $M = \Sigma_{i=1}^{n} m_i$ is the total weight of the JuR, C and K are the damping and stiffness of the single degree of freedom system, $\tau_{dc}(t)$ is the total torque on motor shafts, and $p_j^\star(t)$ is the displacement of the hull. The total effect of the load (including the wave, wind, current and external loads) is:

$$\tau_d(t) = \tau_{wave}(t) + \tau_{wind}(t) + \tau_{current}(t) + \tau_{ex}(t). \quad (3)$$

The displacement of the hull is calculated by

$$p_j^\star(t) = R\theta(t) \quad (4)$$

where R expresses the effective radius and $\theta(t)$ is the angular of the pinion. From Eqs. (2) and (4), the JuR's hull kinematics are written as:

$$Rs^2\theta(s)\sum_{i=1}^{n} m_i + RCs\theta(s) + KR\theta(s) = \tau(s). \quad (5)$$

Similarly, the differential Dynamic Amplification Factor (DAF) of a damped JS reacting to a step load is calculated using the ratio of the dynamic response to the static response. There are always variables at play that affect reality. Therefore, errors caused by fluctuations in DAF values would have an impact on the actual location of the Rig's hull.

$$p_j^\star(t) = DAF.\, p_{jp}^\star(t) \quad (6)$$

The displacement DAF subjected to a step load is, therefore, [20]:

$$DAF(t) = \frac{p_j^\star(t)}{p_{jp}^\star(t)} = 1 - e^{-\xi\omega_n t}\left(\cos\omega_n\sqrt{1-\xi^2 t} + \frac{\zeta\sin\omega_n\sqrt{1-\zeta^2 t}}{\sqrt{1-\zeta^2 t}}\right), \quad (7)$$

where $\zeta = (0.05 - 0.2)$ is the damping ratio of the system. The decoupling system approach divides the system into subsystems with the same transfer function, for the ease and simplicity of embedded control and simulation. Then, by substituting DAF = 0.6284 into Eq. (6), we get $p_j^\star(t) = 0.6284p_{jp}^\star(t)$, $\dot{p}_j^\star(t) = 0.6284\dot{p}_{jp}^\star(t)$, $\ddot{p}_j^\star(t) = 0.6284\ddot{p}_{jp}^\star(t)$. Using Laplace transform with initial conditions, $p_j^\star(0) = 0$, $\dot{p}_j^\star(0) = 0$ we get

$$0.6284^2Ms^2p_{jp}^\star(s) + 0.6284^2Csp_{jp}^\star(s) + 0.6284^2Kp_{jp}^\star(s) = \tau(s). \quad (8)$$

The displacement of the hull is calculated by

$$p_{jp}^\star(s) = R\theta(s), \quad (9)$$

with $k_e = 1/R$ is the inverted factor in rotary – translational drive. Finally, the equation describing the transfer function of the kinematics of JS is written as:

$$G_{JuR} = \frac{\theta(s)}{\tau(s)} = \frac{k_e}{0.6284^2Ms^2 + 0.6284Cs + 0.6284K} \quad (10)$$

CONTROL THE JS OVER THE NETWORK USING FUZZY-PSO STRATEGY

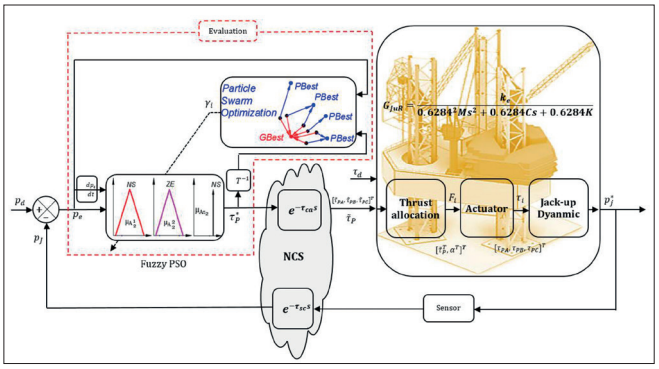

Fig. 2. The proposed structure for the JS of the JUR

As a similar type of networked control system (NCS), the insight diagram of the FPSO control through the network is presented in Fig. 2. The fuzzy system includes the double-inputs p_e, dp_e/dt, and single-output $\tau^\star$ [7], and the fuzzy rule comprises a set of IF-THEN forms within θ^i:

$$\text{If } \sigma_1 \text{ is } K_1^i,\ldots, \sigma_n \text{ is } K_n^i \text{ then } \tau^\star \text{ is } \theta^i \tag{11}$$

Therein, K_1^i, $K_2^i \ldots K_n^i \in R^h$ and are the input variables and output variables of the fuzzy system [7], respectively. By using the fuzzy system with the fuzzy rule (11), the Max-Prod inference rule, the singleton fuzzifier, the product inference engine and centre average defuzzifier, the output response $\tau^\star$ is defined as follows:

$$\tau^\star(\sigma) = \frac{\sum_{i=1}^{m} \theta^i [\prod_{j=1}^{n} \mu_{K_j^i}(\sigma_j)]}{\sum_{i=1}^{m} [\prod_{j=1}^{n} \mu_{K_j^i}(\sigma_j)]} \tag{12}$$

for $\mu_{K_j^i}(\sigma)$ expresses the membership functions (MFs) with m as the number of fuzzy rules. We get

$$T^{\star T} = [\bar{\tau}^{\star 1}, \bar{\tau}^{\star 2},\ldots, \bar{\tau}^{\star m},]^T \in R^m \tag{13}$$

as the vector of the fuzzy parameter. The fuzzy basis functions with ϕ are written as

$$\phi_i(\sigma) = \frac{\sum_{i=1}^{m} \theta^i [\prod_{j=1}^{n} \mu_{K_j^i}(\sigma_j)]}{\sum_{i=1}^{m} [\prod_{j=1}^{n} \mu_{K_j^i}(\sigma_j)]} \tag{14}$$

and notate $\phi_i(\sigma) = [\phi_1(\sigma), \phi_2(\sigma),\ldots, \phi_m(\sigma)]^T$ as the fuzzy basis function vector. Then, the fuzzy system (12) is able to represent the linear parametric form as:

$$\tau^\star(\sigma) = T^T \phi(\sigma). \tag{15}$$

Lemma 1 [21]: Let $\varphi(\sigma)$ be a continuous function defined on a compact set $\Omega \subset R^n$. Then, for any constant $\xi < 0$, there exists a fuzzy system $\tau^\star(\sigma)$ in the form of Eq. (12), as

$$sup_{\sigma \in \Omega} \mid \varphi(\sigma) - T^{\star T} \phi(\sigma) \mid \leq \xi \tag{16}$$

By *Lemma 1*, the nonlinear function $\varphi(\sigma)$ can be approximated as

$$\phi(\sigma, T^\star) = T^{\star T} \phi(\sigma). \tag{17}$$

Define

$$T^{\star\star} = \arg\min_{T^\star \in \Omega} [\sup_{x \in Z} \mid \phi(\sigma) - \phi(\sigma, T^\star) \mid] \tag{18}$$

where Z and Ω are compact regions for σ and $T^\star$, respectively. Consequently, the minimum approximation error is determined as:

$$\xi = \phi(\sigma) - T^{\star\star T} \phi(\sigma). \tag{19}$$

The demonstration in [21] indicates that the control system is asymptotically stable with the *Lemma 1* after attaining Eq. (19). PSO is tasked with identifying the appropriate fuzzy set parameters that meet the requirements within Remark 1 and Remark 2 below:

Remark 1: Finding convergence for the best algorithms is a time-consuming task. There are several parameters that need to be tuned as the computing speed rapidly decreases.

Remark 2: The optimal parameter quality depends on the number of generations and the fitness function value $f_{FP}(t)$. If a small value is used, the convergence value is local. However, in the case of using the large value, the processing time will be slow.

Consequently, in order to increase processing speed (Remark 1) and ensure optimal parameter quality (Remark 2), a limit function approximates the goal value in Eq. (20) for quality relative to the target but, also, in a smaller space and with fewer occurrences. The fitness function value and the number of individuals are guaranteed, as in Eq. (21) and (22).

$$\lim_{t \to \infty} \| \tilde{f}_{FP} = \lim_{t \to \infty} \| f_{FP}^0 - f_{FP} \| = 0 \tag{20}$$

Concerning the relation between the importance of fitness and iteration constraints [22], the fitness function value and the number of individuals are guaranteed, as in Eq. (21) and (22).

$$iter_m^{min} \leq iter_m \leq iter_m^{max} \tag{21}$$

$$f_{FP}^{min} \leq f_{FP} \leq f_{FP}^{max} \tag{22}$$

In particular, PSO aims to identify the best MFs value, in order to help increase processing speed. Therefore, Algorithm 1 is used to make decisions regarding coefficient γ_i based on the PSO algorithm [10], in order to enhance control quality in a time-varying situation.

Algorithm 1: Dynamically learned PSO algorithm for proposed FPSO

Initialise the position $\gamma_i^p(l)$ and the velocity $v_i(l)$ randomly.
Initialise correction coefficient γ_i $(\gamma_1, \gamma_2, \gamma_3, \gamma_4)$.
while $iter_m^{min} \leq iter_m \leq iter_m^{max}$ **do**
  for each iteration l **do**
    update the profits of $\gamma_{i,j}^p(l)$ and $\gamma_{i,j}^{Gb}(l)$ using Eqs. (23) and (24)

$$\gamma_{i,j}^p(l+1) = \begin{cases} \gamma_{i,j}^p(l), if\ J\left(\gamma_{i,j}^p(l+1)\right) \geq J\left(\gamma_{i,j}^p(l)\right) \\ \gamma_{i,j}^p(l+1), \quad otherwise \end{cases} \tag{23}$$

$$\gamma_{i,j}^{Gb}(l+1) = argmin_{\gamma_{i,j}^{Pb}} J\left(\gamma_{i,j}^{Pb}(l+1)\right), 1 \leq i \leq s \tag{24}$$

    initialise the particle attribute $v_i(k)$ using Eq. (25)

$$v_{i,j}(l+1) = w(k) v_{i,j}(l) + c_1 r_1 \left[\gamma_{i,j}^{Pb}(l) - \gamma_{i,j}^p(l)\right] + c_2 r_2 \left[\gamma_j^{Gb}(l) - \gamma_{i,j}^p(l)\right] \tag{25}$$

    for

$$w(g) = \frac{(iter_{max} - g)(w_{max} - w_{min})}{iter_{max}} + w_{min} \tag{26}$$

    determine a new point $\gamma_{i,j}^p(l)$ using Eq. (27)

$$\gamma_{i,j}^p(l+1) = \gamma_{i,j}^p(l) + v_{i,j}(l+1) \tag{27}$$

    use the new coefficient $\gamma_{i,j}^p(l)$ to correct the amplitude profits of the MFs, then define a fitness condition according to Eq. (28).

$$f_{FP}(t) = \int_0^\infty t |p_e(t)| dt \text{ guaranteed fitness constraints } f_{FP}^{min} \leq f_{FP} \leq f_{FP}^{max} \tag{28}$$

    compare the latest profits of the MFs to the termination condition. If the convergence condition is not satisfied, increase l and go back to Step 5.
  end
end

The implementation of particle swarm optimisation (PSO) is simple and computationally effective. In our scenario, the membership functions' centres, widths, and weights are contained in the particles. The dimension of particles is determined by the number of parameters. The PSO is applied off-line to tune the membership functions. The FPSO

performance is defined as:

$$\tau_P^{\star}(\sigma) = \frac{\Sigma_{i=1}^{m}\theta^i[\Pi_{j=1}^{n}\mu_{K_{\gamma j}^i}(\sigma_j)]}{\Sigma_{i=1}^{m}[\Pi_{j=1}^{n}\mu_{K_{\gamma j}^i}(\sigma_j)]}, \quad (29)$$

where $\mu_{K_{\gamma j}^i}(\sigma_1) = [\gamma_1(K_1^1, K_1^2, \ldots K_1^j)]$ expresses the error fuzzy set $p_e(t)$, $\mu_{K_{\gamma j}^i}(\sigma_2) = [\gamma_2(K_2^1, K_2^2, \ldots K_2^j)]$, indicates the error-velocity fuzzy set dp_e/dt, and $\theta_\gamma^i = [(\gamma_3 + \gamma_4/s)(\theta^1, \theta^2, \ldots \theta^i)]$ are the so-called 'output fuzzy set' $\tau_P^{\star}(\sigma)$. Then, $\phi_\gamma(\sigma) = [\phi_\gamma^1, \phi_\gamma^2, \ldots, \phi_\gamma^m] \in R^m$ represents the fuzzy basis vector as

$$\phi_\gamma(\sigma) = \frac{[\Pi_{j=1}^{n}\mu_{K_{\gamma j}^i}(\sigma)]}{\Sigma_{i=1}^{m}[\Pi_{j=1}^{n}\mu_{K_{\gamma j}^i}(\sigma)]}. \quad (30)$$

The PSO algorithm modifies the values of the fuzzy set with coefficient $\gamma_i(\gamma_1, \gamma_2, \gamma_3, \gamma_4)$ to define the best correction coefficient γ_i. An extremely high value of the control force might cause an imbalance in the JuR's overall energy system. The issue of energy consumption must be addressed, to achieve optimal management, and our goal is to use the least amount of energy possible while also boosting the amount of continuous electric supply that is required. In light of this, the desire may be summarised as follows [22]:

$$Maximise(\alpha_{uc}\vartheta_{\tau^{\star}Pc} + \alpha_{es}\vartheta_{es}) \in [0,1], \quad (31)$$

where $\vartheta_{\tau^{\star}Pc}$ is the stable electric coefficient and ϑ_{es} is the energy savings coefficient. $\alpha_{\tau^{\star}Pc}$ and α_{es} define weights for stable electric and energy saving, respectively, setting $\alpha_{\tau^{\star}Pc} + \alpha_{es} = 1$. Hence, the increase ϑ_{es} is proportional to the decrease in energy consumption U_e:

$$\vartheta_{es} \propto \frac{1}{U_e}. \quad (32)$$

The gains in energy savings can be expressed as [22]:

$$\vartheta_{es}(\tau^{\star}_P) = \left(1 - \left(\frac{U_0 - U_{min}}{\Delta U}\right)^2\right) \in [0,1]. \quad (33)$$

Obviously, the energy system should guarantee that optimal condition (U_0) approaches the lowest possible energy consumption and ϑ_{es} increases, resulting in the greatest energy savings. In other words, we want to find U_0 values that will give the optimisation function in Eq. (33) the best value possible. However, higher values of $\tau_{P0}^{\star}(\sigma)$ will result in a loss in the energy component, i.e. higher values of $\tau_{P0}^{\star}(\sigma)$ causes $U_0 \to U_{max}$ and, thus, $\frac{U_0 - U_{min}}{\Delta U} \to 1$, which results in losing the gain in the energy component. Equation (33) achieves our intended goal of balancing stable electric and energy consumption. The constraints are specified as:

$$0 \le U_{min} \le U_0 \le U_{max}. \quad (34)$$

Related to the time-delay problem, the response of the NCS will be lowered by the network-induced delay, causing errors in the data transmission process $e^{-d_{ca}s}$ [27-28]. Typically, the delay of the control signal d_{ca} transmits to the JuR dynamic model. Therefore, the signal $\tilde{\tau}_P(\sigma)$ of the FPSO controller transmits information over the network as follows:

$$\tilde{\tau}_P(\sigma) = \tau^{\star}{}_P(\sigma)e^{-d_{ca}s} \quad (35)$$

The sensor-to-controller delay causes an error in the JS response ($e^{-d_{ca}s}$), giving

$$p_j(s) = p^{\star}{}_j(s)e^{-d_{ca}s} \quad (36)$$

From Eqs. (35) and (36), the problems of d_{sc} and d_{ca} reduce the quality of the jacking system control over the network. So, the control force and torque vectors at each truss leg are rewritten as

$$\tilde{\tau}_P = [\tilde{\tau}_{PA}, \tilde{\tau}_{PB}, \tilde{\tau}_{PC}]^T \quad (37)$$

The control signals of each actuator consist of two components: amplitude and direction of force. The control force vectors from the thrust allocation to the actuator are determined as follows:

$$F_i = [\tilde{\tau}_P^T, \alpha^T]^T \in \mathbf{R}^{2r} \quad (39)$$

EXPERIMENTAL MODEL DESIGN

MECHANICAL POWERTRAIN AND EMBEDDED SYSTEM DESIGN

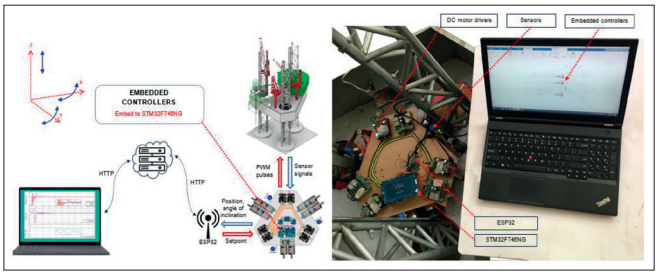

Fig. 3. Fig. 3. Overall structure of UT-JuR 01

The position state variable of the JuR-hull served as the foundation for the experimental model, identified as UT-JuR 01, and is described in detail in Fig. 3. This integrated controller compares the instantaneous position signal to the desired position, to determine the incorrect location. The controller then uses the inaccurate number as a starting point to calculate the motor's lifting force to raise the JuR-hull to the designed position. The main components and functions of the UT-JuR 01 model are as follows:

- The 24 VDC power supplies voltage power to the control modules. A 24 VDC to 5 VDC voltage converter was used to power the STM32F746NG and ESP32 central processors, a 24 VDC to 3.3 VDC voltage converter to power the sensor block (IMU MPU6050 and Encoder), and a 24 VDC to 12 VDC voltage converter to power the DC Drivers block.
- The mounted IMU sensor monitored the platform inclination while the displacement sensor (Encoder) measured the location of the JuR-hull at the legs. The central processor STM32F746NG received feedback signals through an ADC converter circuit. Besides this, the supervisor station received the feedback values from the NCS via the ESP32 module.

- The central processor STM32F746NG computed the control force values based on the errors between the desired position and the actual position. This control signal was converted to a PWM pulse, to manage the speed and direction of the DC motors (via the DC Drivers) and to raise and lower the JuR-hull to the desired position.

CONTROL ALGORITHM

The testing control process in the UT-JuR 01 was performed in accordance with Algorithm 2. The ESP32 module received the feedback signal of the JuR's real position throughout this process and sent the data it contained to the supervisor station over the network. The supervisor station, on the other hand, employed the HTTP protocol to retrieve data.

Algorithm 2: Control over the network

Initialise JuR desired position p_d, inclination angle, speed and bit number of data transfer.
Initialise collection date of set-points (ESP32: Position and angle of inclination).
Initialise disturbance filter.
while *Desired position* **do**
  for each *control cycle* **do**
    (a) Determining position erroneous p_e.
    (b) Using the Fuzzy PSO strategy to compute the control force $\tau_p^*(\sigma)$.
    (c) Converting the output control signal to PWM pulse for DC motors.
    (d) Defining the JuR actual position p_J using sensors (Encoder, IMU, distance).
    (e) Transferring the JuR operation data to the cloud (ESP32: Position and inclination angle).
    (f) Comparing the latest JuR position p_J to the termination condition p_d. If the JuR position is not satisfied, increase *control cycle* and go back to Step 6.
  end
end

SIMULATION AND EXPERIMENTAL EVALUATION

SIMULATION RESULTS

In order to evaluate the efficacy of the suggested approach, this paper performed and compared simulations between the FPSO controller and the fuzzy controller [24], utilising the TamDao05 JuR model parameters that were used in this work at 1:100 scale. Matlab 2019a software was also used to simulate the controller and was developed using the same ambient variables and jacking system specifications [14], with reference to the environmental effect factors. Using the *m.file* that connects to Simulink, the PSO algorithm finds the fuzzy controller's optimum, to have the best convergence on the control.

The response time of the JuR employing the FPSO controller is faster than the FC by approximately 3.5 s, in the case of the simulation without environmental influences (shown in Fig. 4(a)). Additionally, the fluctuation amplitude is around 0.12 cm less than the conventional solution. The comparable results indicate that the FPSO solution satisfies the criteria and this controller can guarantee the JuR model's high response quality in NCS circumstances. Besides this, the JuR-hull position's stability under changing weather conditions in the case of the JS is guaranteed by the FPSO controller. Figure 4(b) demonstrates that employing the proposed FPSO results in fluctuations that are 0.22 cm lower and 3.4 seconds faster than when using the FC controller. The performance of the jacking system using the FC controller meets the control requirements, in the case without environmental impacts, but does not achieve the requirements in the case with environmental impacts. However, the FPSO gave a satisfactory performance in all simulation scenarios.

Tab. 1. A response comparison of several controllers for simulation outcomes.

Simulation scenarios	Response time		Fluctuation		Overshoot	
	Fuzzy	FPSO	Fuzzy	FPSO	Fuzzy	FPSO
0 cm – 10 cm	5.5 s	3.5 s	0.45 cm	0.22 cm	4.0 cm	4.5 cm
0 cm – 30 cm	7.0 s	4.5 s	0.50 cm	0.25 cm	5.5 cm	6.5 cm
0 cm – 30 cm – 60 cm	6.5 s	4.5 s	0.55 cm	0.35 cm	6.0 cm	6.5 cm

In circumstances when the truss body was elevated and lowered by 0-10 cm (scenario 1), 0-30 cm (scenario 2), and 0-30-60 cm (scenario 3), Table 1 displays the comparative findings (scenario 3). The FPSO solution responds faster than the original FC approach [24], with response times of 2.0 s, 2.5 s, and 2.0 s for scenarios 1, 2, and 3, respectively. Besides this, the fluctuation amplitude of the FPSO solution is 0.22 cm, 0.25 cm, and 0.35 cm in three scenarios, which is lower than the case of using an FC controller, thereby verifying the quality of the proposed solution. Positive results indicate that the

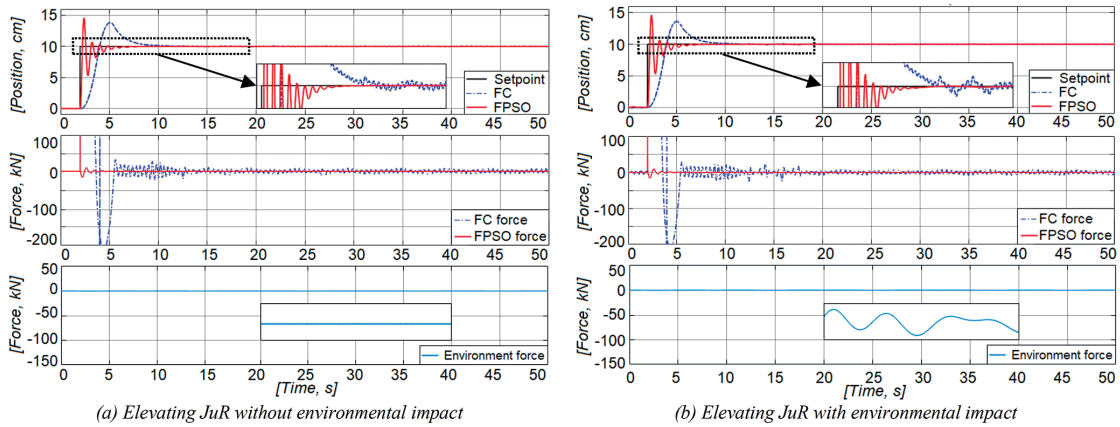

(a) Elevating JuR without environmental impact *(b) Elevating JuR with environmental impact*

Fig. 4. FPSO controller simulation results compared with FC using control over the network

proposed approach offers better response quality than the FC controller due to the optimal correction coefficient. The FPSO approach with the energy consumption function restrictions (34), guarantees that the cost overshoot value is always within allowable limits when the network control environment influences the control process and causes errors $e^{-d_{ca}s}$, $e^{-d_{sc}s}$. Last but not least, the proposed controller FPSO can adapt to the environmental impact by optimal adjustment of the control parameter (the coefficient γ_i). However, the proposed algorithms need to test other actual conditions, in order to verify the advantages in the future.

RESULTS

Testing of the UT-JuR 01-embedded experimental model was carried out in two scenarios, the operating parameters of the UT-JuR 01 were updated online (to the database using the ESP32 module), and the supervisory station continuously retrieved data to synthesize commands. The obtained experimental results are shown in Fig. 5 and Fig. 6. The experimental process was carried out in the two scenarios below:

- Scenario 1: The jacking lifts the JuR-hull from position 0 cm to 30 cm and maintains status in 580 seconds;
- Scenario 2: The JuR-hull is raised to a position of 60 cm from the reference position of 30 cm and maintains status in 580 seconds.

The fluctuation amplitude of the low JuR's legs is 1.35 cm (4.5%) for case 1 and 1.25 cm (2.1%) for case 2. Consequently, the results show that the FPSO solution, controlled via NCS, meets the quality requirements of 6%. The response time for the first case is 120 s and 135 s for the second case. The minimum response time for fluctuation stopping reaches the

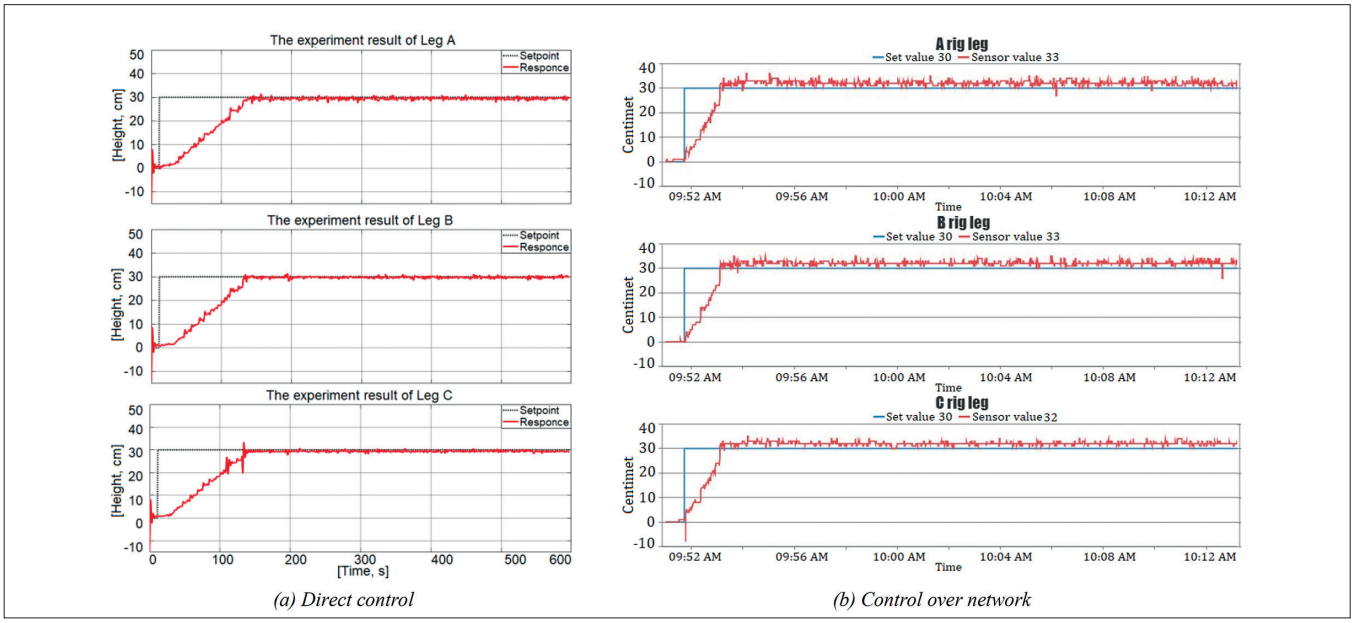

(a) Direct control *(b) Control over network*

Fig. 5. Results of an experiment to move the JuR from a position of 0 cm to 30 cm

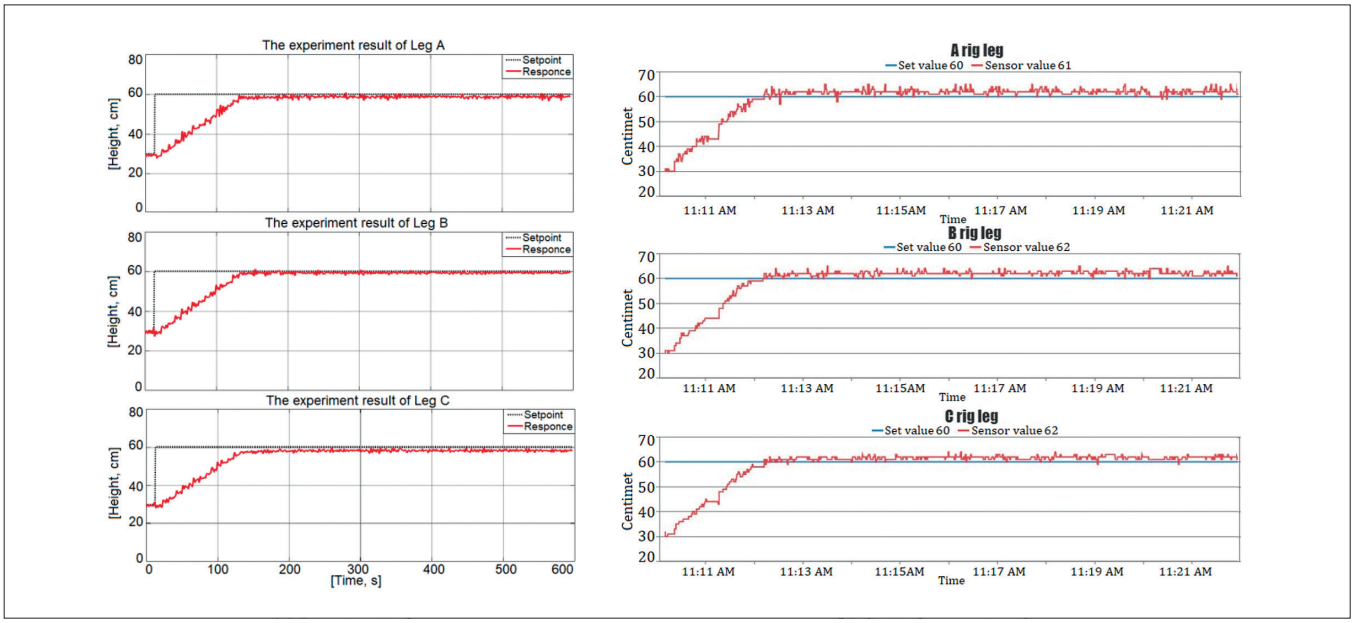

Fig. 6. Results of an experiment to move the JuR from a position of 30 cm to 60 cm

equilibrium value in 4.0 to 5.0 s, in experimental cases within the allowable limit (5.5 s). The direct control test (Figs. 5a and 6a) and over network control (Figs. 5b and 6b) yield identical findings.

Tab. 2. A response comparison of several solutions for experimental outcomes.

Experimental scenarios	Solution		Leg A	Leg B	Leg C	Centre of JuR
30–60 cm	Direct control Control network	over	59.55 60.60	59.75 60.85	59.60 61.05	59.65 60.65
30–80 cm	Direct control Control network	over	79.25 80.65	79.35 81.20	79.30 81.25	79.25 81.15

NB: All measurements are in cm

Table 2 provides further information comparing the testing scenario (30-60 cm and 30-80 cm) response outcomes for leg position and rig centre, while carrying out further control of the model using the network, demonstrating the precision of the data transfer technique used to operate the rig over the network. To meet the quality requirements, the position divergence amplitude, comparing the direct control and the networked control of the 30-60 cm scenario, is between 0.45 cm and 1.10 cm. In the 30-80 cm scenario, position divergence amplitude is between 0.85 cm and 1.40 cm. Compared to direct control, control over network outcomes guaranteed the quality of the system's reaction. Furthermore, the response exhibits duplicated values (displayed as a straight line) at some locations due to the slow speed of data transfer and delays.

CONCLUSION

This paper includes a brief discussion of the JuRs' system design, particularly in the jacking system. Employing an analysis of the JuR's motions along the axis, the mathematical modelling of the jacking system is developed. Additionally, it is thought that the PSO algorithm is a suitable approach for fuzzy adaptive control systems, to improve the performance of the fuzzy controller. Evidence of the proposed FPSO's simulation and experimental performance compared with the Fuzzy controller in the case of the control-induced network, showed the enhanced flexibility and stability of the approach. By using mathematical justifications, the energy system would do well to ensure that the optimal condition (U_0) approaches the lowest possible energy consumption; Eq. (33) achieves our goal of balancing stable electricity and energy consumption. Finally, the UT-JuR 01 model's experimental validation of the problem of energy conservation has not yet been completely tested and evaluated, despite careful analysis.

REFERENCES

1. J.T. Yi, F. Liu, T.B. Zhang, Z.Z. Qiu, and X.Y. Zhang, "Determination of the ultimate consolidation settlement of jack-up spudcan footings embedded in clays," Ocean Eng., vol. 236, pp. 1-13, 2021, doi: 10.1016/j.oceaneng.2021.109509.

2. Q. Yin, J. Yang, G. Xu, R. Xie, M. Tyagi, L. Li, X. Zhou, N. Hu, G. Tong, C. Fu, and D. Pang, "Field experimental investigation of punch-through for different operational conditions during the jack-up rig spudcan penetration in sand overlying clay," J. Petroleum Sci. Eng., vol. 195, pp. 1-21, 2020, doi: 10.1016/j.petrol.2020.107823.

3. F. Wang, W. Xiao, Y. Yao, Q. Liu, and C. Li, "An Analytical Procedure to Predict Transverse Vibration Response of Jack-Up Riser under the Random Wave Load," Shock and Vibration, vol. 2020, pp. 1-9, 2020, doi: 10.1155/2020/5072989.

4. Y. Xie, J. Huang, X. Li, X. Tian, G. Liu, and D. Leng, "Experimental study on hydrodynamic characteristics of three truss-type legs of jack-up offshore platform," Ocean Eng., vol. 234, pp. 1-15, 2021, doi: 10.1016/j.oceaneng.2021.109305.

5. M. Pająk, L. Muślewski, B. Landowski, and A. Grządziela, "Fuzzy Identification of the Reliability State of the Mine Detecting Ship Propulsion System," Polish Marit. Res., vol. 26, no. 1, pp. 55-64, 2019, doi: 10.2478/pomr-2019-0007.

6. M. Pashna, R. Yusof, Z.H. Ismail, T. Namerikawa, and S. Yazdani, "Autonomous multi-robot tracking system for oil spills on sea surface based on hybrid fuzzy distribution and potential field approach," Ocean Eng. vol. 207, pp.1-11, 2020, doi: 10.1016/j.oceaneng.2020.107238.

7. X.K. Dang, V.D. Do, and X.P. Nguyen, "Robust Adaptive Fuzzy Control using Genetic Algorithm for Dynamic Positioning System," IEEE Access, vol. 8, pp. 222077–222092, 2020, doi: 10.1109/ACCESS.2020.3043453.

8. T. Cepowski, P. Chorab, and D. Łozowicka, "Application of an Artificial Neural Network and Multiple Nonlinear Regression to Estimate Container Ship Length Between Perpendiculars," Polish Marit. Res., vol. 28, no. 2, pp. 36-45, 2021, doi: 10.2478/pomr-2021-0019.

9. R. Zagan, I. Paprocka, M.G. Manea, and E. Manea, "Estimation of Ship Repair Time Using the Genetic Algorithm," Polish Marit. Res., vol. 28, no. 3, pp. 88-99, 2021, doi: 10.2478/pomr-2021-0036.

10. L. Zhang, J. Sun, and C. Guo, "A Novel Multi-Objective Discrete Particle Swarm Optimisation with Elitist Perturbation for Reconfiguration of Ship Power System," Polish Marit. Res., vol. 24, no. s3, pp.79-85, 2017, doi: 10.1515/pomr-2017-0108.

11. X. Gu and Q. Shen, "A self-adaptive fuzzy learning system for streaming data prediction," Information Sci., vol. 579, pp. 623-647, 2021, doi: 10.1016/j.ins.2021.08.023.

12. S. Buzura, V. Dadarlat, B. Iancu, A. Peculea, E. Cebuc, and R. Kovacs, "Self-adaptive Fuzzy QoS Algorithm for a Distributed Control Plane with Application in SDWSN," 2020 IEEE International Conference on Automation, Quality and Testing, Robotics (AQTR), pp. 1-6, 2020, doi: 10.1109/AQTR49680.2020.9129922.

13. T. Vinu, S. Kumaravel, and S. Ashok, "Fuzzy Controller-Based Self-Adaptive Virtual Synchronous Machine for Microgrid Application," IEEE Transactions on Energy Conversion, vol. 36, no. 3, pp. 2427-2437, 2021, doi: 10.1109/TEC.2021.3057487.

14. T.D. Tran, V.D. Do, X.K. Dang, and B.L. Mai, "Improving the Control Performance of Jacking System of Jack-Up Rig Using Self-Adaptive Fuzzy Controller Based on Particle Swarm Optimisation," 8th EAI International Conference, INISCOM 2022, pp. 184–200, 2022, doi: 10.1007/978-3-031-08878-0_13.

15. C. Wu, J. Liu, X. Jing, H. Li, and L. Wu, "Adaptive Fuzzy Control for Nonlinear Networked Control Systems," IEEE Transactions on Systems, Man, and Cybernetics: Systems, vol. 47, no. 8, pp. 2420-2430, 2017, doi: 10.1109/TSMC.2017.2678760.

16. M.B. Kadri and S.M.K. Raazi, "Model Free Fuzzy Adaptive Control for Networked Control Systems," Technology Forces J. Eng. Sci., vol. 2, no. 1, pp. 9-19, 2019.

17. W. Deng, X. Tian, X. Han, G. Liu, Y. Xie, and Z. Li, "Topology optimisation of jack-up offshore platform leg structure," Proc. Inst. Mech. Engineers M, J. Eng. Maritime Environ, vol. 235, no. 1, pp. 165–175, 2021, doi: 10.1177/1475090220928736.

18. Y.F. Fan and J.H. Wang, "Method to evaluate effect of spudcan penetration on adjacent jacket piles," Appl. Ocean Res., vol. 106, pp. 1–14, 2021, doi: 10.1016/j.apor.2020.102436.

19. B. Rozmarynowski and W. Jesien, "Spectral Response of Stationary Jack-Up Platforms Loaded by Sea Waves and Wind using Perturbation Method" Polish Marit. Res., vol.28, no. 4, pp.53-62, 2021, doi: 10.2478/pomr-2021-0049.

20. Z. Chao, H. Hong, B. Kaiming and Y. Xueyuan, "Dynamic amplification factors for a system with multiple-degrees-of-freedom," Earthquake engineering and engineering vibration, vol. 19, no. 2, pp. 363–375, 2000, doi: 10.1007/s11803-020-0567-9.

21. W. Min and Q. Liu, "An improved adaptive fuzzy backstepping control for nonlinear mechanical systems with mismatched uncertainties," Automatika, vol. 60, no. 1, pp. 1–10, 2019, doi: 10.1080/00051144.2018.1563357.

22. I. Ullah and D. Kim, "An Improved Optimisation Function for Maximising User Comfort with Minimum Energy Consumption in Smart Homes," Energies, vol. 10, no. 11, pp. 1818, 2017, doi: 10.3390/en10111818.

23. D.P. Kumar, "Particle Swarm Optimisation: The Foundation," International Series in Operations Research & Management Science, vol. 306, pp. 97-110, 2021, doi: 10.1007/978-3-030-70281-6_6.

24. 24. V.D. Do, X.K. Dang, and A.T. Le, "Fuzzy Adaptive Interactive Algorithm for Rig Balancing Optimisation," International Conference on Recent Advances in Signal Processing, Telecommunication and Computing, pp. 143-148, 2017, doi: 10.1109/SIGTELCOM.2017.7849812.

25. K.S. Ahmed, A.K. Keng, and K.C. Ghee, "Stress and stiffness analysis of a 7-teeth pinion/rack jacking system of an Offshore jack-up rig," Eng. Failure Analysis, vol. 115, pp. 104623, 2020, doi: 10.1016/j.engfailanal.2020.104623.

26. Z.M. Ghazi, I.S. Abbood, and F. Hejazi, "Dynamic evaluation of jack-up platform structure under wave, wind, earthquake and tsunami loads," J. Ocean Eng. Sci., vol. 7, pp. 41-57, 2022, doi: 10.1016/j.joes.2021.04.005.

27. H.D. Tran, Z.H. Guan, X.K. Dang, X.M. Cheng, and F.S. Yuan, "A Normalized PID Controller in Networked Control Systems with Varying Time Delays," ISA Transactions, vol.52, pp. 592-599, 2013, doi: 10.1016/j.isatra.2013.05.005.

28. X.K. Dang, Z.H. Guan, T. Li, and D.X. Zhang, "Joint Smith Predictor and Neural Network Estimation Scheme for Compensating Randomly Varying Time-delay in Networked Control System," The 24th Chinese Control and Decision Conference, pp. 512-517, 2015, doi: 10.1109/CCDC.2012.6244077.

CONTACT WITH THE AUTHORS

Xuan-Kien Dang
e-mail: kien.dang@ut.edu.vn

Artificial Intelligent Transportation Research Group
Ho Chi Minh City University of Transport
Vietnam

Tien-Dat Tran

Artificial Intelligent Transportation Research Group
Ho Chi Minh City University of Transport
Vietnam

Thi Duyen-Anh Pham

Artificial Intelligent Transportation Research Group
Ho Chi Minh City University of Transport
Vietnam

Viet-Dung Do

Artificial Intelligent Transportation Research Group
Ho Chi Minh City University of Transport
Dong An Polytechnic
Vietnam